

# Oscillatory Zonal Flows Driven by Interaction between Energetic Ions and Fishbone-like Instability in CHS

A. Fujisawa, S. Ohshima, A. Shimizu, H. Nakano, H. Iguchi, K. Itoh, S. Okamura, K. Matsuoka, T. Minami, Y. Yoshimura, K. Nagaoka, C. Takahashi, S. Nishimura, M. Isobe, C. Suzuki, T. Akiyama, CHS group

National Institute for Fusion Science, Oroshi-cho, Toki 509-5292, Japan

## Abstract

Nonlinear evolution of magneto-hydro-dynamic (MHD) oscillatory phenomenon driven by the interaction with energetic particles has been studied in CHS using twin heavy ion beam probes. The measurements have provided the fine observation of internal structure of plasma quantities, such as electric field, density and magnetic field distortion during a cycle of the MHD phenomenon. The finding of a new kind of oscillating zonal flow driven by interaction between energetic particles and MHD modes should be emphasized for burning state plasmas since the resultant shear of electric field could reach a sufficiently large level to affect the turbulence transport in burning plasmas of the next generation.

## 1. Introduction

MHD phenomena associated with energetic particles are one of highlighted issues for the coming stage of fusion research of burning plasma since the effect of the fusion-generating  $\alpha$ -particles on the plasma property is anticipated in the burning state. A particular attention has been paid on  $\alpha$ -particle-driven instabilities to degrade the plasma confinement and the plasma stability [1-3]. A number of the phenomena classified into the same category have been already identified in toroidal plasma experiments, *e.g.*, fishbone instabilities [4,5] a variety of phenomena associated with Alfvén modes [6,7], energetic particle modes [8]. On the other hand, nowadays, that the electric field shearing [9] should be an important mechanism to suppress turbulence leading into sudden transition to improved confinement states, such as H-mode [10]. Recently, the time-dependent shearing of zonal flows [11,12] is also well recognized as an important mechanism to regulate the drift-wave turbulence. In addition, the orbit loss of energetic particles should be an important element to generate the electric field shear structure [13,14]. Accordingly, the loss of  $\alpha$ -particles in burning plasma may cause a sudden change of the plasma confinement by generating structured electric field [15]

In Compact Helical System (CHS), a toroidal helical device, a MHD phenomenon of quasi-periodic bursts induced by the interaction with energetic proton beams, termed here

*CHS-fishbone*, has been known and extensively studied [16-20]. Recent measurements of heavy ion beam probes (HIBPs) show the internal structural evolution in potential, density and fluctuations during the phenomenon. The paper presents the results of the fine measurements to show a causal linkage between magnetic field distortion and density gradient during a fishbone cycle, and the formation of oscillatory zonal electric field or flow due to the orbit loss of high-energy particles driven by the magnetic field distortion of CHS-fishbone.

## 2. CHS Device and CHS-Fishbone

CHS is a toroidal helical device with a major radius of 1.0 m and an averaged minor radius of 0.2 m. The confinement magnetic field has rotational symmetry with toroidal and poloidal periods of  $m/n=2/8$ , and is characterized by a strong reversed shear across the whole plasma. The device, CHS, is equipped with two heavy ion beam probes (HIBPs) [21] located by 90 degree apart in toroidal position. Both HIBPs can observe the potential and density at the ionization point simultaneously from the beam energy change and detected beam intensity  $I_D$ , respectively. In a sufficient low-density regime, the local density variation can be evaluated roughly as  $\delta n_e/n_e \sim \delta I_D/I_D$ .

CHS-fishbone is a cyclic burstic phenomenon observed in neutral beam (NB) heated plasma for a wide range

of CHS configuration in rather lower density regime of  $n_e < 2 \times 10^{19} \text{ m}^{-3}$ . The pattern of the fishbones is dependent on the magnetic configuration and operational conditions such as heating. Figure 1 presents a typical example of CHS-fishbone on which the analyses are carried out in this paper. A signal of magnetic field fluctuation in Fig. 1(a) demonstrates that a series of the burstic activities occur quasi-periodically in a steady state of NBI-sustained phase. The measurements of magnetic pick-up coils have shown that the

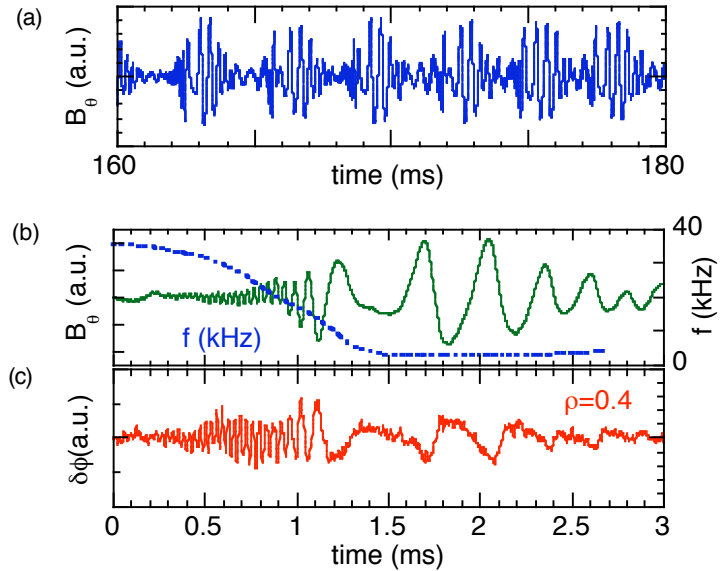


Figure 1: An example of CHS fishbone instability.

(a) Magnetic field evolution including 6 cycles.

(b) A cycle of CHS fishbone, with a curve to show the change of frequency, and (c) potential fluctuation at normalized radius of  $\rho \sim 0.4$ .

underlying mode has  $m=2/n=1$  property, where  $m$  and  $n$  represent poloidal and toroidal mode number, respectively. The conditions to give the fishbone patterns in Fig. 1 are as follows. The magnetic field strength is 0.9 T, and the total injected power of hydrogen NB-heating is approximately  $\sim 800$  kW, with the particle energy being  $\sim 40$  keV. The line average density of the produced hydrogen plasma is  $n_e=0.8 \times 10^{19} \text{ m}^{-3}$ , and the beam driven current is approximately  $\sim 5$  kA in the steady state.

A special feature of the phenomenon in the present experimental condition is that the frequency chirping phase ( $0 < t < \sim 1.3$  ms) is followed by the second or post-cursor phase ( $t > \sim 1.3$  ms) of low frequency ( $\sim 2$  kHz), as is shown in Fig. 1(b). In the chirping phase the underlying mode propagates in ion diamagnetic direction, while the mode propagates in electro-diamagnetic direction in the second phase. Figure 1(c) shows a raw signal of the potential fluctuation (HIBP). Obviously, the potential fluctuation measured with HIBP is well correlated with magnetic field fluctuation, particularly in the chirping phase. In the present analysis, a signal is divided into three parts, as  $F = \langle F \rangle + \Delta F + \delta F$ , where  $\langle F \rangle$ ,  $\Delta F$  and  $\delta F$  represent the temporal average, slowly developing part in the scale of a millisecond and fluctuation part in faster time scale, respectively. The slowly developing parts of density and potential are found to change in response to the nonlinear evolution of magnetic field structure during a cycle of the fishbone

### 3. Oscillatory Zonal Flow Generation during a Cycle of CHS Fishbone

Twin HIBP measurements have been carried out to clarify the detailed evolution of the internal structure during a cycle of the fishbone. The evolution of a radial profile of potential fluctuation amplitude can be evaluated from the data taken shot-by-shot by changing the HIBP observation point. The poloidal angles of the observation points are almost constant during this radial scanning. Figure 2 shows the profiles of potential fluctuation amplitude at times during a cycle of the fishbone, together with the phase difference between the fluctuations of the local potential and a magnetic field pick-up coil outside the plasma. The profiles of amplitude and phase are calculated as conditional averages for 6-7 identical cycles. In this procedure, the fluctuation amplitude at a moment is evaluated using a wavelet analysis [22]. Note that the fluctuation amplitude shown in this paper is an integration around the temporal frequency of the mode with the band-width of  $\pm 8$  kHz.

As is shown in Fig. 2(a), the potential fluctuation amplitudes have two peaks around  $\rho \sim 0.0$  and  $\rho \sim 0.6$  in the chirping phase. The existence of the peak at  $\rho \sim 0.6$  could be consistent with the  $m=2$  property since the radial position corresponds to  $q=2$  rational surface. On the other hand, the presence of the central peak should be contradictory with the

$m=2$  property, since it is expected for  $m=2$  mode to obey  $\delta\phi = \langle E_r \rangle \xi \sim \langle E_r \rangle r^{m-1} = \langle E_r \rangle r$  in the vicinity of the magnetic axis. Here,  $\xi$  and  $\langle E_r \rangle$  denote the magnetic field displacement from the unperturbed magnetic flux surface and mean radial electric field, respectively. Therefore, the appearance of the central peak could be ascribed to the different origin from  $m=2$  distortion of magnetic field. The clear difference observed in the phase between the local potential and a magnetic field fluctuation outside should support this hypothesis. The intermediate region should be regarded as the transient layer between two different regions. In other words, the potential fluctuation should be driven by two different causes. In fact, the twin HIBP measurements show that the potential fluctuation inside the transient layer has  $n=0$  characteristic, while the outside potential fluctuation does  $n=1$  characteristic. If it is assumed that the potential on the magnetic field is constant, the  $n=0$  property should be equivalent to that of  $m=0$ . Therefore, the potential fluctuation in the core region should be symmetric around the magnetic field axis.

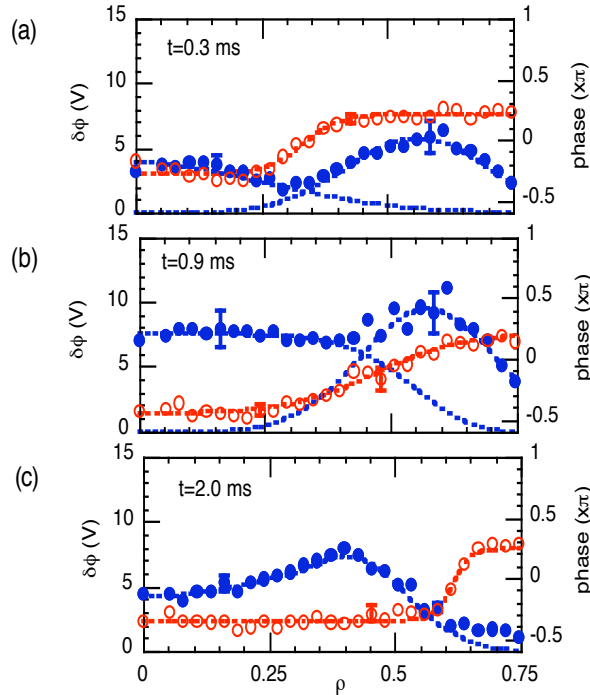


Fig. 2 Profiles of potential fluctuation amplitude and the phase referred to magnetic field pickup coil outside. (a) Those at  $t=0.3$  ms, (b) at  $t=0.9$  ms, and (c)  $t=2.0$  ms. The analysis shows that the potential fluctuations are divided into two components; core fluctuations ( $m=n=0$ ) and that around  $q=2$  surface at  $\rho=0.6$  ( $m=2/n=1$ ).

Under the hypothesis that the potential fluctuation should consist of two different modes of  $m=0$  and  $m=2$ , the spatial structure of the potential fluctuation,  $\delta\phi$ , can be expressed as  $\delta\phi \equiv \delta\phi(\rho) \exp(i\delta_M) = \delta\phi_{m=0}(\rho) \exp(i\delta_{m=0}) + \delta\phi_{m=2}(\rho) \exp[i(\delta_{m=2} + 2\theta)]$ , where  $\theta$ ,  $\delta\phi_{m=0}$  and  $\delta\phi_{m=2}$  represent the poloidal angle coordinate, the local amplitudes of the  $m=0$  and  $m=2$  modes, respectively. The parameters  $\delta_M$ ,  $\delta_{m=0}$ , and  $\delta_{m=2}$  are the phase shifts to the signal of magnetic pick-up coil. Both fluctuation amplitudes,  $\delta\phi_{m=0}(\rho)$  and  $\delta\phi_{m=2}(\rho)$ , can be deduced by solving the above equation, since the parameters  $\phi$ ,  $\delta_M$ ,  $\delta_{m=0}$  and  $\delta_{m=2}$  are provided from the measurement. Examples of the reconstructed mode profiles for  $m=0$  and  $m=2$  are shown by dashed lines in Figs. 2(a) and 2(b) for the cases of  $t=0.3$  and  $0.9$  ms.

Figure 3 shows the reconstructed image of the evolution of the potential fluctuations represented by the equi-contours, together with the radial profiles of potential and electric field fluctuation amplitudes of the  $m=0$  component. From Fig. 3(a), the  $m=2$  potential fluctuation starts to grow then induces the  $m=0$  fluctuation. After the zone of  $m=0$  fluctuation expands with the evolution of the  $m=2$  mode in the chirping phase, the  $m=0$  pattern becomes predominant in the observable range of the HIBP in the post-cursor phase. Figures 3(b) and 3(c) show the details of the development of the  $m=0$  component. In Fig. 3(b), it is easily recognized that the potential fluctuation amplitude around the center,  $\delta\phi_{m=0}(\rho)$ , is almost constant in the chirping phase, hence, the corresponding fluctuation of radial electric field (or flow) is localized in a radial zone ( $0.2 < \rho < 0.6$ ), as is shown in Fig. 3(c).

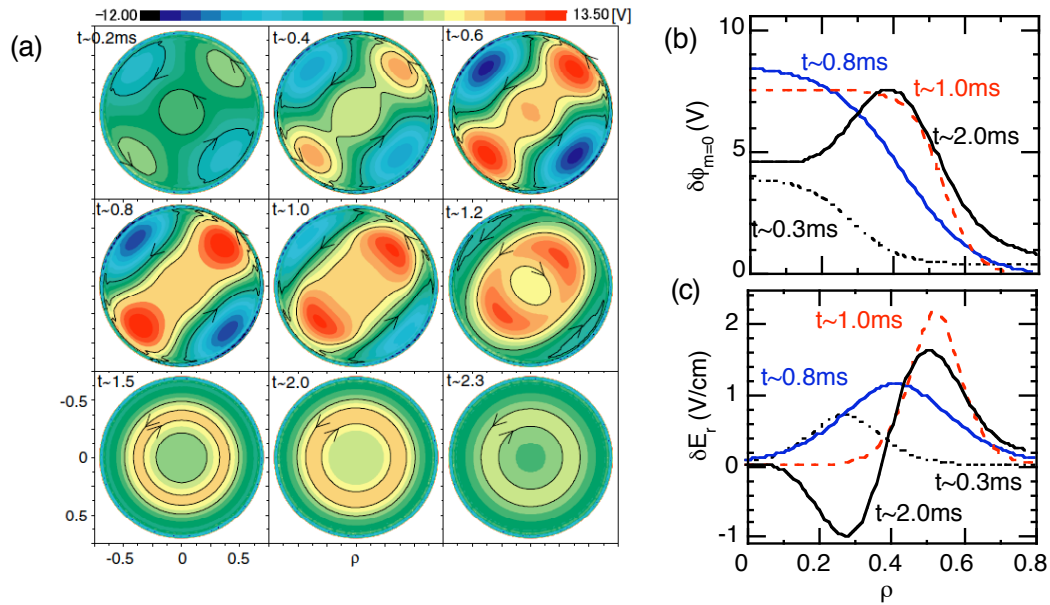


Figure 3 (a) Reconstructed 2D-image plots of potential fluctuation or perturbed flow pattern evolution during a cycle;  $t=0.2, 0.4, 0.6, 0.8, 1.0, 1.2, 1.5, 2.0$ , and  $2.3$  ms. The equi-potential contours are equivalent to the fluctuating EXB-flow pattern. (b) The evolution of potential fluctuation ( $m=0$  part) during a cycle of the fishbone. (c) The evolution of the zonal flows (electric field fluctuation amplitude of  $m=0$  mode).

In Fig. 3(c), a prominent feature of this oscillatory electric field in the chirping phase is its absence of a *double layer* property created by a charge movement, although the electric field finally grows into oscillating zonal structure. The initial *single layer* property can be produced only from direct charge loss, not a charge replacement between the neighboring regions, hence, the oscillatory electric field should be caused by the synchronized change in the energetic particle loss with magnetic field distortion.

Rough estimation of necessary current to induce the electric field oscillation can be made from neoclassical theories. In a toroidal helical plasma, the radial electric field is determined by the neoclassical current being balanced with ion orbit loss current  $\delta j_b$  in this situation. The balance can be expressed by  $\delta j_b + (\partial j_{\text{neo}} / \partial E_r) \delta E_{r,m=0} = 0$ , where  $j_{\text{neo}}$  means the neoclassical current. In a calculation in the case of CHS geometry, the partial derivative is estimated as  $\partial j_{\text{neo}} / \partial E_r \sim 2 \text{ A/kVm}$ . The oscillating electric field in the observation is  $\delta E_{r,m=0} \sim 0.2 \text{ kV/m}$ , therefore, the necessary change in the total orbit loss current  $\delta I_{\text{loss}}$  is evaluated as  $\delta I_{\text{loss}} \sim 2 \text{ A}$ . This is within a plausible range for the present experiment.

#### **4. Mutual Interaction Between Magnetic Field Structure and Energetic Particles and during a cycle of CHS fishbone**

As for the  $m=2$  mode, the degree of magnetic field distortion can be estimated from the amplitude of the potential fluctuation. If it is assumed the plasma resistivity is sufficiently low to keep the potential on the same magnetic flux constant, the observed potential fluctuation should be caused by the distortion of the magnetic flux surface. Consequently, the magnetic field displacement from the undisturbed flux surface can be estimated as  $\xi = \delta \phi_{m=2} / \langle E_r \rangle$ . The evaluated profile of the displacement is shown in Fig. 4(a). The result demonstrates that the displacement grows with its maximum being located around  $q=2$  surface at  $\rho \sim 0.6$  and reaches its maximum at the middle of the chirping phase. The distortion is found to almost disappear in the post-cursor phase ( $t > \sim 1.3 \text{ ms}$ ) within the observable range of the HIBPs.

On the other hand, the signal of the HIBP beam intensity allows us to evaluate how the density profile evolves during a cycle of the fishbone using the first-order approximation with the assumption of neglecting the path integral effect. However, in the low-density regime of this experimental condition, the contribution of the energetic particles (here proton of a dozen keV range) to the ionization of the probing beam particles may not be neglected. Therefore, the change in the detected beam current with HIBPs can reflect the heating beam particle movement to a certain degree. Figure 4(b) shows the slowly developing part of density (or actually detected beam current) at several times as a function of radial coordinate. The results clearly demonstrate that the density deviation propagates outwards in response to the evolution in a cycle of the fishbone. It should be notified that the probe measurement on the plasma edge suggests the outward movement of the beam particles in the case of similar quasi-periodic bursts occurring in other CHS magnetic configuration [20].

In order to clarify the relation between the density gradient and growth of the  $m=2$  mode, a quantity is introduced to indicate the local change of the density gradient,

$\zeta(\rho) = -\partial(\Delta I_b / \langle I_b \rangle) / \partial \rho$ . Figure 4(c) shows the comparison between the position of the maximum of  $\zeta$  and the magnetic field displacement at  $\rho=0.6$ , or  $\xi(\rho=0.6)$ , due to the  $m=2$  mode. The comparison between the temporal evolution of  $\rho(\zeta^{\max})$  and  $\xi^{\max}$  indicates that the plasma distortion due to the  $m=2$  mode appears to take the maximum approximately when the position  $\rho(\zeta^{\max})$  almost agrees with the  $q=2$  rational surface ( $\rho \sim 0.6$ ). Here,  $\rho(\zeta^{\max})$  means the position of the maximum  $\zeta$ . It is obvious that the  $m=2$  mode evolves as the local density gradient increases. It is important to note, again, that the local density gradient here may reflect that of the energetic particle pressure.

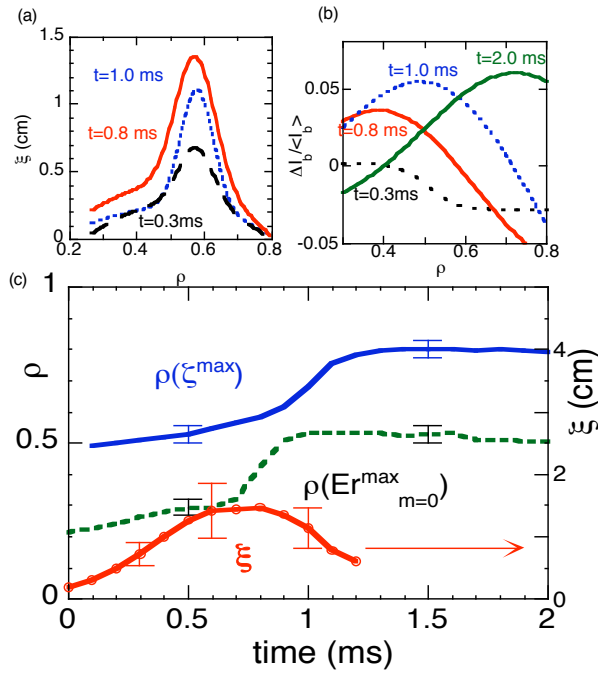


Fig. 4 (a) Evolution of plasma distortion associated with the  $m=2$  mode during the chirping phase. (b) Local gradient change in density profile evaluated from secondary detected current. (c) Plasma distortion  $\xi(\rho = 0.6)$ , density gradient  $\rho(\zeta^{\max})$  and radial positions of electric field maximum  $\rho(E_{r,m=0}^{\max})$  are plotted as a function of time during a cycle of the fishbone, indicating the causal linkage between three quantities.

On the other hand, the maximum of  $\delta E_{r,m=0}$  is also plotted as a function of time, which is denoted by  $\rho(\delta E_{r,m=0}^{\max})$  in the same graph. The comparison indicates that both structural change of density and oscillating electric field move outward in response to the growth of the  $m=2$  mode. The fact shows their causal relationship between  $\rho(\zeta^{\max})$  and  $\rho(\delta E_{r,m=0}^{\max})$  through the evolution of the  $m=2$  mode. These observations deduce a possible scenario for the evolution of the fishbone cycle as follows. The increase in the energetic particles destabilizes the  $m=2$  mode first, then move themselves outwards through the mutual interaction with the mode. The outward movement results in the increase in the beam pressure gradient around the  $q=2$  surface to cause further destabilization of the mode, which simultaneously enhances the loss of the energetic particles to generate the oscillatory zonal flows. As the energetic particles are passed away from the  $q=2$  resonant surface with their loss continuously contributing to generation of the zonal flows, the  $m=2$  mode turns to be stabilized finally. Then, the beam pressure increases to repeat the same process again.

## 5. Summary

In summary, the twin HIBP measurements in CHS have revealed successfully the spatio-temporal evolution of internal structures of electric field, density and plasma distortion during a periodic MHD phenomenon. The observation clearly demonstrates that these structures evolve concomitantly and interactively with each other. The most important observation is a new kind of oscillating zonal flow generated, not via the turbulent Reynolds stress, but from the ion orbit loss current induced by the mutual interaction between energetic particles and the MHD mode. The finding gives a hint of the reduction of background turbulence or the change of transport characteristics by the zonal flow generation from the interaction between  $\alpha$ -particles and their driven MHD-instabilities in the state of plasma burning.

## References

- [1] W. W. Heidbrink, Nucl. Fusion **34**, 535 (1994).
- [2] K. L. Wong, Plasma Phys. Control. Fusion **41** R1 (1999)
- [3] L. Chen et al., Phys. Plasma **1** 1519 (1994).
- [4] K. McGuire et al., Phys. Rev. Lett. **50** 891 (1983).
- [5] L. Chen, R. B. White, M. N. Rosenbluth, Phys. Rev. Lett. **52** 1122 (1984).
- [6] C. Z. Cheng and M. S. Chance, Phys. Fluids **29** 3695 (1986).
- [7] K. L. Wong et al., Phys. Rev. Lett. **66** 1874 (1991).
- [8] F. Zonca, S. Briguglio, L. Chen et al, Phys. Plasma **9** 4939 (2002).
- [9] K. Itoh and S-I. Itoh, Plasma Phys. Control. Fusion **38** 1 (1996).
- [10] F. Wagner et al., Phys. Rev. Lett **49** 1408 (1982).
- [11] P. H. Diamond et al., Plasma Phys. Control. Fusion **47**, R35 (2005).
- [12] A. Fujisawa et al., Phys. Rev. Lett. **93** 165002 (2004).
- [13] Sanae-I. Itoh and K. Itoh, Phys. Rev. Lett **60** 2276(1988).
- [14] K. C. Shaing and E. C. Crume, Jr., Phys. Rev. Lett **63** 2369(1989).
- [15] K. L. Wong et al., Nucl. Fusion **45** 30 (2005).
- [16] S. Sakakibara et al., Jpn. J. Appl. Phys. **37** 252 (1995).
- [17] T. Kondo et al., Nucl. Fusion **40** 1575 (2000).
- [18] K. Toi et al., Nucl. Fusion **40** 1349 (2000).
- [19] M. Isobe et al., Nucl. Fusion **46** S918 (2006).
- [20] K. Nagaoka et al., Phys. Rev. Lett. **100** 0650065 (2008).
- [21] A. Fujisawa et al., Rev. Sci. Instrum. **67** 3099 (1996).
- [22] B. Ph. van Milligen, et al., Phys. Plasmas **7** 3017 (1995).